

UNCLASSIFIED  
AD 425951

DEFENSE DOCUMENTATION CENTER  
FOR  
SCIENTIFIC AND TECHNICAL INFORMATION  
CAMERON STATION, ALEXANDRIA, VIRGINIA



UNCLASSIFIED

NOTICE: When government or other drawings, specifications or other data are used for any purpose other than in connection with a definitely related government procurement operation, the U. S. Government thereby incurs no responsibility, nor any obligation whatsoever; and the fact that the Government may have formulated, furnished, or in any way supplied the said drawings, specifications, or other data is not to be regarded by implication or otherwise as in any manner licensing the holder or any other person or corporation, or conveying any rights or permission to manufacture, use or sell any patented invention that may in any way be related thereto.

425951

MEMORANDUM

RM-2628-PR

DECEMBER 1963

CATALOGED BY DDC  
AS AD NO.

# A NUMERICAL TECHNIQUE FOR SOLUTION OF MULTIDIMENSION HYDRODYNAMIC PROBLEMS

R. Bjork, N. Brooks and R. Papetti

PREPARED FOR:

UNITED STATES AIR FORCE PROJECT RAND

---

The **RAND** Corporation  
SANTA MONICA • CALIFORNIA

---

**MEMORANDUM**

**RM-2628-PR**

**DECEMBER 1963**

**A NUMERICAL TECHNIQUE FOR  
SOLUTION OF MULTIDIMENSION  
HYDRODYNAMIC PROBLEMS**

**R. Bjork, N. Brooks and R. Papetti**

This research is sponsored by the United States Air Force under Project RAND—contract No. AF 49(638)-700 monitored by the Directorate of Development Planning, Deputy Chief of Staff, Research and Development, Hq USAF. Views or conclusions contained in this Memorandum should not be interpreted as representing the official opinion or policy of the United States Air Force.

**DDC AVAILABILITY NOTICE**

Qualified requesters may obtain copies of this report from the Defense Documentation Center (DDC).

---

*The* **RAND** *Corporation*

1700 MAIN ST • SANTA MONICA • CALIFORNIA

PREFACE

This Memorandum documents a numerical procedure which was devised to solve the problem of hypervelocity impact and which was subsequently revised for application to the problem of cratering and ground shock from a nuclear surface burst.

The RAND Symposium on High-Speed Impact, held in 1955, focused attention on a forthcoming Air Force need for information relative to hypervelocity impact. In fact, this symposium was the first of a series of six symposia sponsored jointly by the Air Force, Army, and Navy on the same topic since that date.

At the first symposium, technical data were presented which strongly suggested that the hypervelocity-impact process was hydrodynamic in nature, involving the substantial compression of even the strongest materials, leading to shocks and severe fluid distortion in the resulting flow. The problem was hopelessly complicated from the analytical point of view, and at that time, numerical techniques did not exist which were adequate to provide the desired solutions. The numerical procedure discussed in this Memorandum was devised specifically to attack this problem.

Once developed, the method proved to have application to an area of Air Force interest not contemplated in the original research, namely cratering and ground shock induced by a nuclear surface burst. The procedure has been applied to this problem, and the results are documented in RM-2300, Cratering From a Megaton Surface Burst.

### SUMMARY

This Memorandum discusses in detail a numerical method for solving the compressible, hydrodynamic equations under the limitations of (1) two space dimensions, (2) the inviscid approximation, and (3) the adiabatic approximation. The method allows for the occurrence of shocks, contact discontinuities, and interfaces. Under a proper prescription of initial and boundary conditions, the method generates solutions including the above physical phenomena.

The basis of the method is the extension to two space dimensions of the particle-in-cell (PIC) concept first proposed by Harlow for a one-dimensional computational scheme. The PIC concept involves mass points moving in a Lagrangian sense through an Eulerian space grid. Besides mass, the points carry with them the proper amount of momentum, kinetic energy, and internal energy.

The computational method approximates a set of partial differential equations containing terms in addition to those of the compressible, hydrodynamic equations under the approximations cited. The terms are qualitatively suggestive of thermal conductivity and viscosity but are not exactly analogous to them. The terms are responsible for the computational stability of the numerical method, since they smear shock fronts over a few grid spaces.

The evaluation of errors due to these terms and those of higher order has not as yet yielded to analysis. The errors have been evaluated by comparing numerical solutions with analytical solutions of test problems and with numerical solutions of one-dimensional problems.

The computational scheme contains a feature known as "grid-changing," which permits optimum resolution of all phases of the problem using the limited memory capacity of present-day electronic computers.

prob-  
in-

CONTENTS

PREFACE .....	11
SUMMARY .....	
• LIST OF SYMBOLS .....	1
Section •	
I. INTRODUCTION .....	
II. PROBLEM DESCRIPTION .....	
System of Equations to be Solved .....	
Initial and Boundary Conditions .....	
III. QUALITATIVE DESCRIPTION OF THE METHOD .....	
Integration Technique .....	1
Discussion of Errors .....	2
Grid Changes .....	
IV. DETAILED DESCRIPTION OF THE METHOD .....	2
Physical Example .....	2
Representation of the Fluid .....	2
Initial Conditions .....	3
Equation of State .....	3
Preliminary Calculation of Velocity .....	3
Preliminary Calculation of Internal Energy .....	3
Mass Movement .....	4
Repartitioning .....	4
Pressure Calculation .....	5
Stability Check .....	5
Grid Change .....	5
REFERENCES .....	5



CONTENTS

PREFACE .....	iii
SUMMARY .....	v
• LIST OF SYMBOLS .....	ix
Section •	
I. INTRODUCTION .....	1
II. PROBLEM DESCRIPTION .....	3
System of Equations to be Solved .....	3
Initial and Boundary Conditions .....	3
III. QUALITATIVE DESCRIPTION OF THE METHOD .....	9
Integration Technique .....	9
Discussion of Errors .....	11
Grid Changes .....	21
IV. DETAILED DESCRIPTION OF THE METHOD .....	23
Physical Example .....	23
Representation of the Fluid .....	25
Initial Conditions .....	30
Equation of State .....	31
Preliminary Calculation of Velocity .....	35
Preliminary Calculation of Internal Energy .....	38
Mass Movement .....	43
Repartitioning .....	49
Pressure Calculation .....	50
Stability Check .....	50
Grid Change .....	53
REFERENCES .....	59

SYMBOLS

- e = specific internal energy
- g = gravitational acceleration
- P = pressure
- t = time
- u = radial component of particle velocity
- $\vec{u}$  = particle vector velocity
- V = volume
- v = axial component of particle velocity
- $v_s$  = velocity of sound
- x = radial coordinate
- y = axial coordinate
- $\varphi$  = stress power
- $\Phi$  = potential of the external force field
- $\Psi$  = total specific energy,  $e + \frac{1}{2} \vec{u} \cdot \vec{u}$

## I. INTRODUCTION

In recent times, many important physical problems that demand the solution of the compressible hydrodynamic equations, using more than one space dimension, have arisen. Two examples are the ground motion in the early stages of a nuclear ground burst and the motion induced when a projectile strikes a target at extremely high velocities. It might seem curious that although both problems involve solid media, the hydrodynamic equations are used to describe the phenomena. However, this is precisely the approximation found necessary in the high-pressure, high-density regions encountered in these processes.

The solutions of this class of physical problems generally feature the presence of shocks, which are allowed in the framework of the nonlinear partial differential equations. Across these shocks, discontinuities in the dependent variables occur. The complications which arise in the analytical treatment of shocks are generally very great. For this reason a great deal of effort has been devoted in the past to the formulation of schemes that yield numerical solutions on electronic computers. Because of these complications, most of the work in the past has been confined to problems which contain a single space variable. This in turn implies the existence of a strong spatial symmetry, usually plane, spherical, or cylindrical.

However, in the case of solids, the presence of a free surface often has an extremely important influence on physical behavior. Such a free surface amplifies the complexity of the already difficult

analytical treatment to such a degree that workers in the field despair of attaining analytical solutions by the use of presently known techniques. A free surface also increases the complexity of the numerical solutions in that it demands the use of more than one space dimension, and its presence usually leads to severe distortion of the medium.

At the time that this work was undertaken, it was evident that the numerical analogue of the Lagrangian formulation broke down when severe distortion of the medium occurred and that the analogue of the Eulerian formulation contained spurious material-diffusion terms whenever the problem included free surfaces and interfaces. The technique described in this Memorandum circumvents these two difficulties. Furthermore, it has been successfully applied to the hypervelocity-impact problem<sup>(1)</sup> and to the early motion of the ground during a nuclear surface burst.<sup>(2)</sup>

The example chosen for describing the method is that of the air flow following a nuclear airburst. It should be emphasized that this problem has not yet been solved by the method, and that difficulties that prevent its solution may arise. However, this problem contains some generalizations not required in the problems that have been solved, thereby allowing a more complete discussion to be given. These are the presence of an external body force (gravity) and a nonhomogeneous medium (the exponentially varying atmosphere).

## II. PROBLEM DESCRIPTION

### SYSTEM OF EQUATIONS TO BE SOLVED

The numerical method is designed to solve the hydrodynamic equations with the inviscid, adiabatic approximation. The representation of these equations in Eulerian coordinates takes the following form:

$$\rho \frac{D\vec{u}}{Dt} + \text{grad } P + \rho \text{ grad } \Phi = 0 \quad (1)$$

$$\rho \text{ div } \vec{u} + \frac{D\rho}{Dt} = 0 \quad (2)$$

$$\frac{De}{Dt} - \frac{P}{\rho} \frac{D\rho}{Dt} = 0 \quad (3)$$

$$P = P(\rho, e) \quad (4)$$

where

$$\frac{D}{Dt} = \frac{\partial}{\partial t} + \vec{u} \cdot \text{grad}$$

The independent variables are the time  $t$ , and a set of spatial coordinates  $\vec{x}$ . The dependent variables are

$\vec{u}$  = particle velocity

$P$  = pressure

$\rho$  = density

$e$  = specific internal energy

The potential  $\Phi$  of the external force field must be specified in advance.

Equation (1), Euler's equation of motion, contains the assumption that the only forces which accelerate the fluid are pressure forces and external forces which may be derived from a potential.

Equation (2), the equation of continuity, is a mathematical statement of the fact that mass must be conserved.

Equation (3) is the first law of thermodynamics under the adiabatic approximation. It states that the only way the internal energy of a fluid element may be changed is through the action of pressure forces during expansion or compression of the element.

Equation (4) is the equation of state of the substance under consideration. It establishes an equilibrium relation (solved explicitly for  $P$ ) between the pressure, density, and specific internal energy of a small element of the material.

Although Eqs. (1) through (4), together with a potential function  $\Phi$  and appropriate boundary and initial conditions, completely specify the motion, they are not in the most convenient form for the particular numerical computations which we have in mind. We therefore transform them in the following way.

The dot product of Eq. (1) with  $\vec{u}$  is taken to obtain

$$\rho \vec{u} \cdot \frac{D\vec{u}}{Dt} + \vec{u} \cdot \text{grad } P + \rho \vec{u} \cdot \text{grad } \Phi = 0 \quad (5)$$

Substitution of Eq. (2) into Eq. (3) yields

$$-\rho \frac{De}{Dt} = P \text{ div } \vec{u} \quad (6)$$

We then use the vector identity

$$\operatorname{div}(\vec{P}\vec{u}) = P \operatorname{div} \vec{u} + \vec{u} \cdot \operatorname{grad} P$$

together with Eq. (6), to obtain

$$\vec{u} \cdot \operatorname{grad} P = \operatorname{div}(\vec{P}\vec{u}) + \rho \frac{De}{Dt} \quad (7)$$

Equation (7) is substituted into Eq. (5). The result is

$$\rho \frac{D}{Dt} \left( \frac{1}{2} \vec{u} \cdot \vec{u} + e \right) + \operatorname{div}(\vec{P}\vec{u}) + \rho \vec{u} \cdot \operatorname{grad} \ddagger = 0 \quad (8)$$

If we integrate Eq. (8) over a region whose volume is  $V$  and whose surface is denoted by  $S$ , we have

$$\int_V \left[ \rho \vec{u} \cdot \operatorname{grad} \ddagger + \rho \frac{D}{Dt} \left( \frac{1}{2} \vec{u} \cdot \vec{u} + e \right) \right] dV = - \int_S \vec{P}\vec{u} \cdot d\vec{S} \quad (9)$$

where Gauss's theorem has been applied to the right-hand side.

Equation (9) is the form which is actually used in the numerical computations, together with Eqs. (1) and (4).

#### INITIAL AND BOUNDARY CONDITIONS

The problems which we wish to solve are transient, nonlinear, initial-boundary value problems in two space dimensions. Their nature is such that if we prescribe initial conditions at time  $t$  and appropriate boundary conditions for all times  $\tau$ , where

$$t \leq \tau \leq t + \Delta t$$

we can find solution fields at a subsequent time  $t + \Delta t$ . As we have stated earlier, such problems do not lend themselves to an analytical treatment, especially when the solution fields contain

a variety of discontinuities such as shocks, slip lines, and free surfaces, as they do in many problems of interest.\*

We are therefore forced to solve difference analogues of the differential equations to obtain solutions at successive points in time.

In order to solve the difference equations at a succession of times it is necessary to have at our disposal the following kinds of data which must be used simultaneously with the difference equations.

#### Initial Data

At some time  $t_0$  values of all of the dependent variables, ( $P$ ,  $\rho$ ,  $e$ ,  $\vec{u}$ ) must be specified at a set of points covering the region of interest. It is not necessary to specify all these quantities at the same set of points. In the numerical scheme which is described later, the velocity, density, and specific internal energy are specified at one set of points, while the pressure is specified at an entirely different set of points. The reason for this will become more evident later.

#### Boundary Data

Boundary-data requirements assume a variety of forms, which depend on the kinds of boundaries that appear in the region we wish to cover by our numerical solution.

---

\* At the present time we have not even the assurance from mathematics that these problems are solvable and contain unique solutions.<sup>(3)</sup> Some assurance is obtained by comparing numerical solutions with physical experiments, with other types of numerical solutions, and with the very few analytical solutions which can be obtained.



First, there are rigid boundaries. The appropriate constraint here is that the normal component of the fluid velocity must coincide with the normal component of velocity assigned to the rigid boundary. If the rigid boundary is fixed in time, then the normal component of fluid velocity must vanish, of course, at this boundary. If a point, axis, or plane of symmetry appears in the problem, it must be treated as a fixed boundary.

A second kind of boundary often encountered is a free surface. At a free surface we must assign zero pressure to the fluid, otherwise it would do work on a vacuum or vice versa.

At interfaces and contact discontinuities the pressure and normal components of fluid velocity must be continuous, while density, internal energy, and tangential components of velocity may change abruptly across such surfaces. In the numerical procedure to be described, no special arrangements need to be made in order to preserve the requisite continuities in pressure and normal velocities. The principal reason for this is that the numerical procedure introduces terms which have the effect of smoothing out discontinuities in the solution fields.<sup>(4,5)</sup> However, because we keep track of each particle in the system, we can still trace out a fairly sharp "interface" which separates wave elements comprised of different materials.

Contact discontinuities can be approximately determined by noticing the distribution of mass points for a single material at a given time.<sup>(6)</sup>

Finally, moving shock surfaces may occur on which the well-known Rankine-Hugoniot conditions must be satisfied. Again, errors

in the numerical procedure tend to replace a shock discontinuity by a zone of finite width across which the dependent variables vary in a rapid, but relatively smooth, fashion. The Rankine-Hugoniot conditions are automatically satisfied by the difference equations governing the motion, so that again no special arrangement must be made for shocks in the numerical procedure.

### III. QUALITATIVE DESCRIPTION OF THE METHOD

#### INTEGRATION TECHNIQUE

The method of solution employs the Particle-In-Cell (PIC) concept devised by Harlow. In Ref. 7 he presents a scheme for solving the equations for the case of plane symmetry, which is a one-dimensional problem. In this Memorandum, the scheme is modified and extended to two dimensions. Harlow has independently extended his method to two dimensions and has applied it to a number of aerodynamic problems.<sup>(k,6)</sup>

A general description of the method is aided by considering the equations under investigation in the form

$$\rho \frac{\partial \vec{u}}{\partial t} + \rho \vec{u} \cdot \text{grad}^* \vec{u} + \text{grad} P + \rho \text{grad} \phi = 0 \quad (10a)$$

$$\frac{\partial \rho}{\partial t} + \vec{u} \cdot \text{grad}^* \rho + \rho \text{div} \vec{u} = 0 \quad (10b)$$

$$\rho \frac{\partial \phi}{\partial t} + \rho \vec{u} \cdot \text{grad}^* \phi + \rho \vec{u} \cdot \text{grad} \phi + \text{div} (\rho \vec{u}) = 0 \quad (10c)$$

where

$$\phi = \frac{1}{2} \vec{u} \cdot \vec{u} + e$$

$$P = P(\rho, e) \quad (10d)$$

An Eulerian grid is laid down, and in this grid many particles are initially positioned. The mass is considered to be concentrated in these particles. During the computation, these particles move throughout the grid, carrying with them mass and momentum as well

as internal and kinetic energy. Since the particles move in a Lagrangian sense throughout an Eulerian grid, the method may be said to incorporate some features of both formulations. The dependent variables, viz., density, velocity, pressure, and specific internal energy, are always specified at the Eulerian grid points.

In solving the equations, initial and necessary boundary conditions are set up. The differential equations are then integrated with respect to time. Thus the essential problem is, given the variable fields at time  $t$ , to find the new fields at time  $t + \Delta t$ . The computation proceeds in two steps. In the first, the convective terms (starred in Eqs. (10a) through (10c)) are neglected, and the truncated set of differential equations is approximated in finite difference form. From these it is possible to obtain new tentative values of velocity and specific internal energy,  $\tilde{u}$  and  $\tilde{e}$ , respectively.

In the second step, the mass points are moved, using the average of the old and the tentative new velocity. After the mass movement, a calculation is made to determine which masses have changed cells. If no masses enter a cell during this time cycle, the tentative values are accepted as the final values.

When one or more masses enter a cell, a process known as repartitioning is carried out. The particle is first considered to have brought with it an amount of momentum, given by the product of its mass and the velocity of the cell which it left. This momentum is added to that of the cell the mass entered, and a new velocity for that cell is determined by dividing the total new momentum by

the total new mass. The new velocity is taken to be the final velocity for this particular time cycle; and the new total mass, the final mass. In addition, a mass entering a cell is assumed to have brought with it an amount of internal energy, given, similarly, by the product of its mass and the specific internal energy of the cell which it left. This is added to the internal energy of the cell which the mass entered.

It is readily shown that the repartitioning process does not conserve kinetic energy if the velocity of the cell which the particle entered is different from that which it left. When the momentum and internal energy are conserved in this way, some kinetic energy is always lost. That is, the estimated kinetic energy assigned to the cell after mass movement but before repartitioning is always greater than the kinetic energy of the cell after repartitioning. In order to conserve total energy, the loss of kinetic energy is arbitrarily added to the internal energy of the cell in which this kinetic-energy defect occurred. The mass movement and subsequent repartitioning process simulates the convective terms neglected in the first step.

#### DISCUSSION OF ERRORS

A thorough discussion of PIC errors would include the determination of a single set of difference and differential equations which correspond to the PIC process, the establishment of the convergence of PIC solutions to solutions of the fluid-dynamic equations and their initial and boundary data, and the establishment of a stability criterion.

At the present time, there appears to be no satisfactory analytical treatment of the PIC convergence and stability characteristics. The greatest effort has been placed on the determination of a set of difference equations which form an analogue to the PIC numerical scheme and on the construction of differential equations that are modeled by this process to first order in the time increment and to second order in the cell widths. (5,6,8)

The derivation of the differential equations which are approximately represented by PIC solutions lies outside of the scope of this Memorandum. Those who are interested in this development may refer to Refs. 4 and 8.

For the present numerical scheme, these differential equations have the following form in cylindrical coordinates with the angular dependence omitted:

$$\frac{\partial \rho}{\partial t} + \frac{1}{x} \frac{\partial x \rho u}{\partial x} + \frac{\partial \rho v}{\partial y} = 0 \quad (\text{continuity})$$

$$\rho \frac{Du}{Dt} + \frac{\partial p}{\partial x} + \rho \frac{\partial \phi}{\partial x} = \frac{1}{x} \frac{\partial}{\partial x} (x \lambda_u \frac{\partial u}{\partial x}) + \frac{\partial}{\partial y} (\lambda_v \frac{\partial u}{\partial y}) \quad (\text{momentum, x direction})$$

$$\rho \frac{Dv}{Dt} + \frac{\partial p}{\partial y} + \rho \frac{\partial \phi}{\partial y} = \frac{1}{x} \frac{\partial}{\partial x} (x \lambda_u \frac{\partial v}{\partial x}) + \frac{\partial}{\partial y} (\lambda_v \frac{\partial v}{\partial y}) \quad (\text{momentum, y direction})$$

$$\rho \frac{De}{Dt} + p \left[ \frac{1}{x} \frac{\partial x u}{\partial x} + \frac{\partial v}{\partial y} \right] = \frac{1}{x} \frac{\partial}{\partial x} (x \lambda_u \frac{\partial e}{\partial x}) + \frac{\partial}{\partial y} (\lambda_v \frac{\partial e}{\partial y})$$

$$+ \lambda_u \left[ \left( \frac{\partial u}{\partial x} \right)^2 + \left( \frac{\partial v}{\partial x} \right)^2 \right] + \lambda_v \left[ \left( \frac{\partial u}{\partial y} \right)^2 + \left( \frac{\partial v}{\partial y} \right)^2 \right] \quad (\text{energy})$$

where

$$\lambda_u = \rho |u| \frac{\Delta x}{2}$$

$$\lambda_v = \rho |v| \frac{\Delta y}{2}$$

In general, boundary-cell analysis does not yield analogues to these differential equations. We see that the error terms, that is the terms which do not coincide with our original equations of motion, formally appear in the above set of equations in the same manner as would the effects of certain physical dissipative mechanisms. This has led to the common usage of the terminology "effective viscosity" and "effective heat conduction" to describe these errors. Moreover, the effects of these errors on the computer solutions have been interpreted as those which would have been caused by an effective viscosity and heat conduction introduced into the difference analogues of the original differential equations. (5,8) In the right-hand side of the analogue momentum equation is to be the divergence of a collection of elements,  $\tau^{ij}$ , and the terms on the right-hand side of the analogue energy equation not containing  $e$  are

---

\* In this section, liberal use of the tensor notation will be made. Thus  $\tau^{ij}$  represents a collection of  $n^2$  elements which transform like the components of a contravariant tensor of rank two;  $u^i$  and  $u_i$  represent the contravariant and covariant elements, respectively, of the velocity vector. A comma is used to denote covariant differentiation, and summation is assumed (unless explicitly stated otherwise) whenever an index is repeated. For instance,  $\varphi = \tau^{ij} u_{i,j}$  is a shorthand for  $\varphi = \sum_{i,j=1}^n \tau^{ij} \left[ \frac{\partial u_i}{\partial x^j} - \sum_{\alpha=1}^n \Gamma_{ij}^{\alpha} u_{\alpha} \right]$  where  $\Gamma_{ij}^{\alpha}$  is the appropriate Christoffel symbol.

to be the stress power,  $\varphi$ , associated with  $\tau^{ij}$

$$\varphi = \tau^{ij} u_{i,j}$$

where the form of neither of these relations is to explicitly depend on the details of the initial and boundary data of the flow problem, then these particular error terms in the analogue equations may be associated with a particular dynamic-stress matrix  $\tau(ij)^*$  given by

$$\tau(ij) = \lambda_{(j)} \frac{\partial u^i}{\partial x^j} \quad i, j = 1, 2 \text{ (no sum on } j)^*$$

$$\tau(3k) = \tau(k3) = 0 \quad k = 1, 2, 3$$

where

$$\lambda_j = \frac{\rho |u^j| \Delta x^j}{2}$$

and

$$\{u^1, u^2, u^3\} = \{u, v, 0\}$$

$$\{x^1, x^2, x^3\} = \{x, y, \theta\}$$

---

\* If the transformation properties of a set of elements are not known, or if they do not satisfy a tensor transformation law, we use the notation  $A(ij)$  rather than  $A^{ij}$ ,  $A_{ij}$ , etc. If a repeated index is not summed, we put parenthesis around it to emphasize this fact. For instance,  $A_{(1)(1)}$  is not summed; however,  $A(ij) B_{ij}$  represents a sum.



From this form for the elements of the matrix  $\tau_{ij}$ , and from their interpretation as elements of a dynamic-stress matrix, the following facts may be immediately derived:

The elements of  $\tau_{ij}$  do not transform like the elements of a contravariant tensor of rank two. Thus, the stress power  $\tau_{ij} u_{i,j}$  is not invariant under admissible coordinate transformations in  $E^3$ . This leads to the result that such physical properties as entropy, specific internal energy, and density at a point will vary with a change of spatial coordinates describing that point. Moreover, the stress vector,  $F^i(p)$ , at a given point  $(p)$  with respect to a surface through the point described by its unit normal vector  $v_j(p)$ , presumably is related to  $\tau_{ij}$  by  $F^i(p) = \tau_{ij} v_j(p)$ . Again, the lack of tensorial property of  $\tau_{ij}$  leads to  $F^i$ 's which depend not only on the surface  $v_i(p)$  but on the particular coordinate system used to describe the position of points in the portion of  $E^3$  under consideration. (This is not surprising, since the entire error analysis leading to the analogue differential equation is valid for one particular coordinate system and no other.)

The established relations for  $\tau_{ij}$  do not leave the flow equations Galilean invariant.\*

By inspection, we see that  $\tau_{ij}$  is not symmetric with respect to interchange of the indices  $i$  and  $j$ . If we perform the usual decomposition into symmetric (S) and antisymmetric (A) parts, we obtain  $\tau_{ij} = \tau_S(ij) + \tau_A(ij)$ . We know that a constitutive relation

---

\* This particular property of the analogue equations has already been recognized by Harlow.<sup>(5)</sup>

corresponding to the viscosity hypothesis will only be related to  $\tau_S(ij)$ . The antisymmetric part  $\tau_A(ij)$  must be accounted for in some other way.

The viscosity hypothesis is  $\tau_S(ij) = C(ijkl) \epsilon_{kl}$  where  $\epsilon_{kl} = \frac{1}{2} [u_{k,l} + u_{l,k}]$  and the C's are symmetrical with respect to interchange of the first two and last two indices. Because  $\tau_S(ij)$  is not a tensor, we avoid the usual representation,  $C^{ijkl}$ , which implies tensorial properties that our coefficients do not have. It is easily shown that for the given form of  $\tau_S(ij)$  the viscosity coefficient  $C(1, 2, 1, 2)$  (and all of those derivable from it by symmetry arguments) must satisfy a set of equations which are inconsistent except on a line given by  $|u^1| \Delta x^1 = |u^2| \Delta x^2$ .

Hence, the origin of  $\tau_S(ij)$  cannot be said to be viscous in nature. If we introduce the most general linear constitutive relation connecting the stress elements  $\tau(ij)$  with the deformation tensor  $\epsilon_{kl}$ ,  $\tau(ij) = B(ijkl) \epsilon_{kl}$ , we still obtain incompatible relations for some of the coefficients of this linear relation. Thus the antisymmetric part of  $\tau(ij)$  (as well as the off-diagonal terms of the symmetric part) cannot be obtained by even the most general linear constitutive relation connecting the stress elements with the deformation tensor  $\epsilon_{ij}$ .

The presence of the antisymmetric elements  $\tau_A(ij)$  adds additional confusion to the attempted representation of errors as physical effects, for it can be shown that a rather arbitrary partitioning among a number of physical effects (couple-stresses, couple density fields, and possibly more general constitutive relations

than we have considered here) may all lead to the same  $\tau_A(ij)$  that is implied by our analogue differential equations. Thus, among other difficulties, there seems to be no unique way of assigning physical effects to the error terms considered.

A similar analysis can be made which starts with the assumption that the remaining error term in the energy equation containing the specific internal energy,  $e$ , may be thought of as the divergence of a heat-flux vector  $\{Q^i\}$ . This analysis also exhibits the many weaknesses of such an assumption. We first observe that the elements of the "pseudo-heat-flux vector"  $Q(i)$ , which are given by  $\{Q(i)\} = \left\{ \lambda_1 \frac{\partial e}{\partial x_1}, \lambda_2 \frac{\partial e}{\partial x_2}, 0 \right\}$ , do not transform like the components of a contravariant vector, with the result that the heat flux, as well as the physical variables, entropy, specific internal energy, density, etc., exhibit the highly undesirable property of changing at a point under admissible coordinate transformations. Another drawback of this assumption is that it implies a heat-conduction law where heat flow is proportional to the gradient of specific internal energy rather than of temperature, a condition which would make physical sense only when  $e$  was just a function of temperature (which in general is not true).

In summary, we may say that the assumption that the errors may be thought of as related to distinct physical effects leads to many contradictions of the assumption. Therefore there seems to be little merit in treating the lowest-order errors induced by a PIC program as anything other than just plain errors.

Although the terms which we have been discussing represent errors, they are largely responsible for the applicability of PIC

as a practical numerical scheme. These elements provide the required smoothing that we need if we do not wish to keep track of shocks which would be expected to appear in the actual solution of the inviscid equations for adiabatic compressive flows.<sup>(9,10)</sup>

As a result of these terms, our solutions exhibit relatively smooth variations in shocked regions, rather than the violent oscillations which would characterize numerical solutions in these same regions when no such elements are present. These artificial smoothing errors are much larger than real dissipative terms which may occur in our physical system. (They must be in order to provide the necessary stabilizing influence.) For this reason, certain precautions must be observed when using this sort of a program. Shocks are smeared out over approximately three grid increments in the numerical solutions, whereas the true shock thickness may occur over a small fraction of a grid increment. Hence, shock thicknesses derived from this sort of program should not be quoted as physically significant results. Also, real dissipative phenomena should not be incorporated into the original equations where the corresponding artificial smoothing effects are many times larger than the real ones.

In many instances, it is possible to replace these artificial smoothing terms by more desirable forms. Such replacements are treated in Ref. 5.

It is easy to show that whenever mass points leave a cell but none enter it, the difference equations for that cell contain neither our previously defined errors nor any convective terms.<sup>(8)</sup>

This particular situation seldom causes any problem in interior cells, but it often arises and persists for many time cycles in cells adjoining a boundary, particularly a free surface in a region of essentially one-dimensional flow. The effects which this situation has on the PIC solution of problems are little understood. It suffices to say here that such cells may contribute a major source of errors in PIC solutions and that these errors may propagate to the interior cells.

Because of the lack of a good error analysis for this kind of numerical scheme, it must be emphasized that the principal evaluation of the results must be based on a comparison of PIC solutions, and mathematical solutions whenever they are available (which is seldom). Other tests, such as checking the sphericity of results (where sphericity is expected) and varying time and space increments in the PIC program to see what happens, are sometimes useful.

An empirical investigation of this kind was used to ascertain the nature and extent of errors incurred by the PIC numerical scheme such as described in this Memorandum, and the following tests were made.

a. Numerical solutions to one-dimensional, uniform-shock-wave problems were solved for a variety of shock strengths and for equations of state of aluminum, iron, tuff, and polytropic gases with gamma equal to 1.4 and 2.0. Numerical results were compared to the simple analytical solutions which in these instances were at our disposal.

b. Numerical solutions to the problems of the one-dimensional rarefaction of air into a vacuum and of compressed tuff into a vacuum were obtained. In each instance the resulting theoretical flows are simple centered waves, which admit analytical solutions. Again the numerical results were compared to these analytical solutions.

c. An axisymmetric numerical solution to a spherical air-burst problem in a uniform atmosphere was computed in cylindrical coordinates and compared to a Lagrangian solution of the same problem by H. L. Brode<sup>(10)</sup> in spherical coordinates.

The results of these tests led to the following set of general qualitative observations which appeared to be consistent with our numerical solutions.

Shock velocities and the estimated position of shock fronts were in good agreement with the corresponding theoretical solutions and with values obtained in Ref. 10. Generally, agreement within  $\pm 5$  per cent was obtained. The estimated position of shock fronts in the numerical solutions was taken to be the point at which the pressure was equal to the arithmetical average of the peak pressure behind the shock zone and the initial pressure. The width of the shock zones varied from two to five cell widths but generally remained around three cell widths in extent.

The largest errors in the solution fields generally occurred immediately behind a shock zone and in regions of very low density where there were very few (generally less than four) mass points per cell. Most often (though this was not always true) the numerical

solution tended to exceed the corresponding theoretical values right behind the shock and then to execute a damped oscillatory motion about the theoretical values. The velocity and specific internal energy generally exhibited smaller errors than did the density and pressure in these regions. Relative errors seldom exceeded 20 per cent and were more often on the order of 5 per cent for reasonable choices of the cell widths and time increments. In the continuous flows (rarefaction solutions) the numerical solutions were very good, often giving relative errors of less than 1 per cent and exhibiting stronger deviations only when regions of very low density were encountered in the tail of the rarefaction for air. (The tuff rarefaction exhibited no tailing off of the density to zero.)

#### GRID CHANGES

For such purely practical reasons as the limited size of the electronic computer's fast memory and the desire to keep the computing time within reasonable bounds, it is possible to use only a limited number of grid points. Consequently, resolution in the solution of two-dimensional problems is very troublesome.

To utilize the resolution to the utmost, an artifice termed a "grid change" has been developed. We take advantage of the fact that the interesting effects expand in size and that the medium outside the motion is undisturbed until some signal from the expanding region reaches it. In the case of hypervelocity impact and nuclear bursts, the exterior fluid is undisturbed until a shock reaches it, and the region of motion is entirely within this

outward-moving shock. Thus, it is only necessary that the grid cover the region of motion and a reasonable amount of undisturbed fluid outside of it. The procedure is to lay down such a grid and constantly test for the slightest indication of motion at the grid's periphery. The computation is stopped when such motion is detected, and a new, somewhat larger grid is laid down for the next phase of the computation, which encompasses some new undisturbed fluid. In this way, the interesting region always occupies a large fraction of the grid points available.



#### IV. DETAILED DESCRIPTION OF THE METHOD

##### PHYSICAL EXAMPLE

In order to illustrate the numerical process, we take as an example a surface explosion in air over a fixed ground in the presence of a uniform gravitational field. The geometric representation selected is one of cylindrical symmetry about the axis  $x = 0$  with the ground at  $y = 0$  as shown in Fig. 1. We treat the air as a perfect gas, so that the equation of state for the fluid is

$$P(\rho, e) = (\gamma - 1)\rho e \quad (11)$$

where  $\gamma$  is a constant usually equal to 1.4. It will be apparent that any equation of state of the form  $P = f(\rho, e)$  may as readily be used. The external force field has a potential

$$\Phi = gy \quad (12)$$

where  $g$  is the gravitational acceleration.

The initial conditions are

$$\vec{u}(\vec{x}, 0) = 0 \quad (13)$$

$$\rho(\vec{x}, 0) = \rho_0 \exp(-y/\lambda) \quad (14)$$

$$\begin{aligned} e(\vec{x}, 0) &= \alpha e_0 \quad (\text{for } x^2 + y^2 \leq r_0^2) \\ e(\vec{x}, 0) &= e_0 \quad (\text{for } x^2 + y^2 > r_0^2) \end{aligned} \quad (15)$$

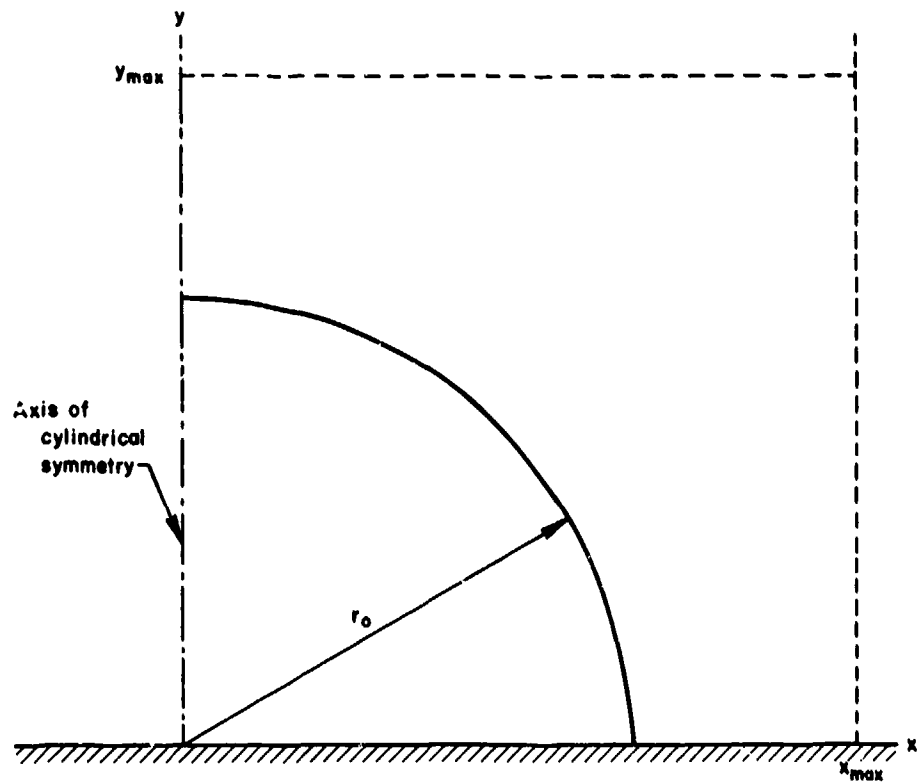


Fig. 1 -- Surface-burst geometry

The particle velocity  $\vec{u}$  is zero at  $t = 0$ ; the density  $\rho$  of the fluid is an exponential function of altitude; the specific internal energy  $e$  is  $e_0$  in the undisturbed area, and a constant  $\alpha$  times  $e_0$  within the disturbed area. The initial pressure is determined by substitution of Eqs. (14) and (15) into Eq. (11), the equation of state.

The boundary conditions to be satisfied are that there is to be no fluid motion across the fixed boundary  $y = 0$  and that the radial component of velocity  $u$  vanishes at  $x = 0$ . These two conditions may be written as

$$v(x, 0, t) = 0$$

$$u(0, y, t) = 0$$

where  $v$  and  $u$  are respectively the axial and radial components of velocity. The fluid is considered to extend indefinitely with increasing  $x$  and increasing  $y$ .

At this point it should be emphasized that the particular representation of the physical problem described above is not necessarily the most realistic model for an extensive investigation of the physical phenomena; rather, it is selected to illustrate the application of the numerical procedure. It is clear that other initial conditions within the disturbed region, other equations of state, other models of the undisturbed medium, and other heights of burst may be used in place of those assumed above.

#### REPRESENTATION OF THE FLUID

The volume is considered to be divided into a finite number of

volume elements, each of which is fixed in position, shape, and size. For our example this region is bounded by  $x = 0$  on the left,  $y = 0$  on the lower side, and extends indefinitely in the direction of increasing  $x$  and  $y$ . Since we wish to maintain a certain degree of resolution, for the time being, we limit the region to a maximum  $x_{\max}$  on the right and  $y_{\max}$  above, as shown in Fig. 1.

One of the volume elements into which the region is subdivided is shown in Fig. 2a. Element  $ij$  is bounded on the left by  $x_{1i}$ , on the right by  $x_{1i+1}$ , on the lower side by  $y_{1j}$ , and on the upper side by  $y_{1j+1}$ . It subtends an angle of one radian about  $x = 0$ . The volume of element  $ij$  is

$$V_{ij} = \frac{1}{2} (x_{1i+1}^2 - x_{1i}^2) (y_{1j+1} - y_{1j}) \quad (16)$$

A convenient notation is that the center of area of the volume element cross section shown in Fig. 2b is at  $x_{2i}$ ,  $y_{2j}$  where

$$x_{2i} = \frac{1}{2} (x_{1i} + x_{1i+1})$$

$$y_{2j} = \frac{1}{2} (y_{1j} + y_{1j+1})$$

and the center of volume is at  $x_{3i}$ ,  $y_{3j}$  where

$$x_{3i} = \sqrt{\frac{x_{1i}^2 + x_{1i+1}^2}{2}}$$

$$y_{3j} = \frac{1}{2} (y_{1j} + y_{1j+1})$$

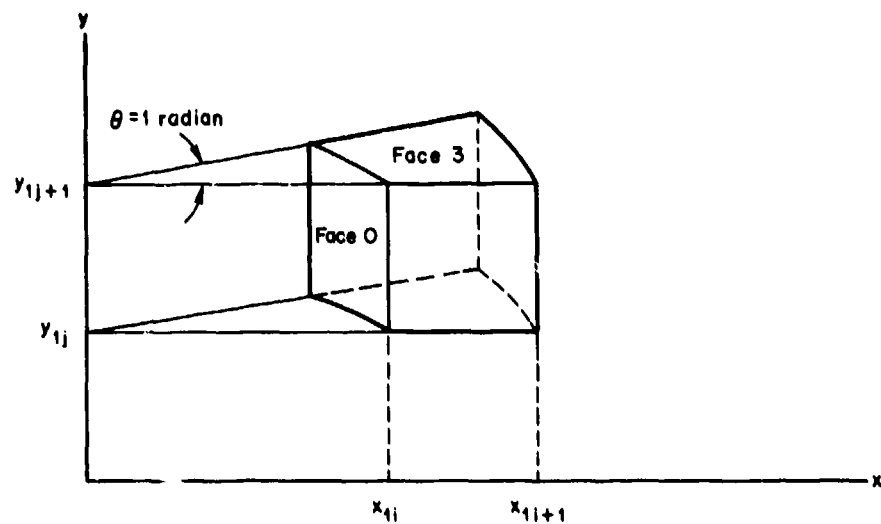


Fig. 2a -- Volume element  $ij$  in cylindrical symmetry

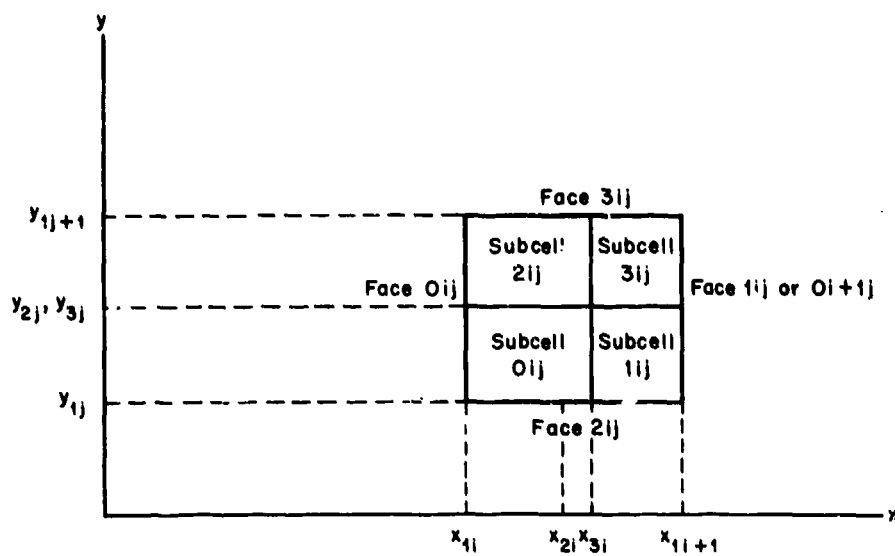


Fig. 2b -- Volume element  $ij$  cross section

Furthermore, the subcells 01j, 11j, 21j, and 31j all have equal volumes.

The fluid in each volume element, or cell, is represented by a number of discrete mass points. These mass points are free to move from cell to cell during the history of the motion. At any instant in time  $t_n$ , the total mass  $M_{1j}^n$  in a given cell is equal to the sum of the values of the discrete masses contained in the cell. With the total mass and the volume of a cell known, the density  $\rho$ , or mass per unit volume, in cell 1j is

$$\rho_{1j}^n = M_{1j}^n / V_{1j} \quad (17)$$

where  $\rho_{1j}^n$  is the density at time  $t_n$ , and  $V_{1j}$  is given by Eq. (16).

Velocity, density, and specific internal energy are properties attached to the cell, and they are considered to be constant over the cell at a particular time. The components of velocity at time  $t_n$  are designated in the x direction by  $u_{1j}^n$ , and in the y direction by  $v_{1j}^n$ ; the specific internal energy  $e$  for cell 1j is  $e_{1j}^n$ .

The pressure  $P$  is measured at points where several volume elements meet. For our example, pressures  $P_{1j}^n$ ,  $P_{1+1j}^n$ ,  $P_{1j+1}^n$  and  $P_{1+1j+1}^n$  are at the respective points  $x_{1j}$ ,  $y_{1j}$ ;  $x_{1+1j}$ ,  $y_{1j}$ ; etc. This is shown in Fig. 3. Pressures at intermediate points are assumed to be given through linear interpolation of nearby pressures. Thus the pressure at a point  $y$  along face 01j is given by

$$P_{01j}^n = P_{1j}^n + \frac{y - y_{1j}}{y_{1j+1} - y_{1j}} (P_{1j+1}^n - P_{1j}^n) \quad (18)$$

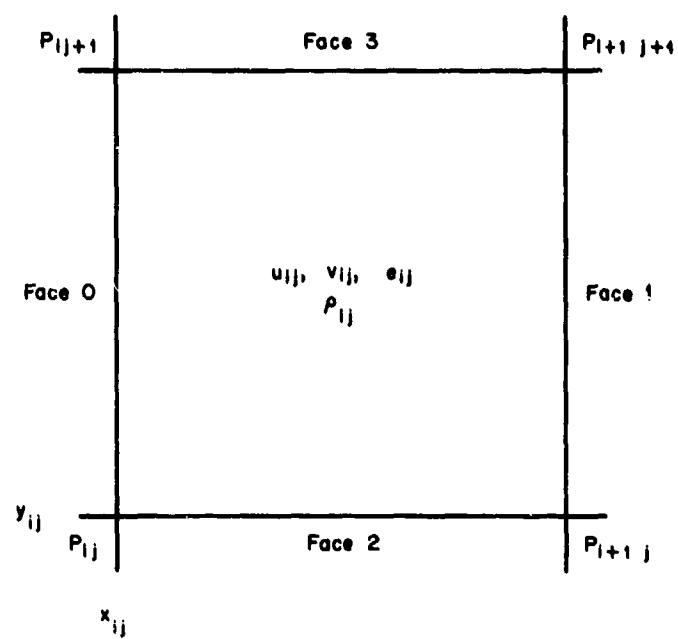


Fig. 3 — The variables of volume element  $ij$

A similar relation applies to each of the other faces 11j, 21j, and 31j.

External forces are treated in much the same manner. We observe that the potential function  $\Phi$  appearing in Eqs. (1) and (9) is always in the form

$$\text{grad } \Phi = \left( \frac{\partial \Phi}{\partial x}, \frac{\partial \Phi}{\partial y}, \frac{\partial \Phi}{\partial z} \right) = (-X, -Y, -Z)$$

where X, Y, and Z are the components of force in the x, y, and z directions, respectively. For our example, gravity is the potential force and its components are

$$\text{grad } \Phi = (0, g, 0) \quad (19)$$

where  $\Phi$  is defined by Eq. (12). In this particular case,  $\text{grad } \Phi$  is a constant.

#### INITIAL CONDITIONS

The mass in a given element of volume is

$$M = \int_V \rho dV \quad (20)$$

If we substitute Eq. (14) for  $\rho$  and  $(x dx dy d\theta)$  for  $dV$  in Eq. (20), the total mass  $M_{ij}^0$  originally in cell ij is

$$M_{ij}^0 = \int_{x_{1i}}^{x_{1i+1}} \int_{y_{1j}}^{y_{1j+1}} \int_0^1 \rho_0 e^{-y/\lambda} x dx dy d\theta$$

which after integration becomes



$$M_{ij}^0 = \frac{\rho_0 \lambda}{2} (x_{11+1}^2 \cdot x_{11}^2) (e^{-y_{1j}/\lambda} - e^{-y_{1j+1}/\lambda}) \quad (21)$$

This mass is divided equally among the mass points originally in the cell. The points in each cell are positioned so that the density is approximately uniform over the volume of the cell. For instance, if there are eight points originally in a given cell, their locations might appear as indicated by the cross marks in Fig. 4. Since the points are free to move from cell to cell as time goes on, it is necessary to record the mass of each point so that the total mass or density in a cell can be determined at any time.

The initial velocity in each cell is zero in the example

$$u_{ij}^0 = 0 \quad (22)$$

The disturbed area, within which the specific internal energy  $e_{ij}^0 = \alpha e_0$ , consists of a number of cells which lie wholly or partially within the radius  $r_0$ . Outside this region,  $e_{ij}^0 = e_0$ .

#### EQUATION OF STATE

Having specified the other initial conditions, we calculate the pressures from the equation of state, Eq. (4). In order to evaluate the pressure, which is a function of density and specific internal energy, it is necessary to define an effective density and specific internal energy for the region immediately surrounding the point at which pressure is computed. Since the density of the fluid is considered to be constant over a cell, we define the mass  $M$  associated with the pressure  $P_{ij}$  as

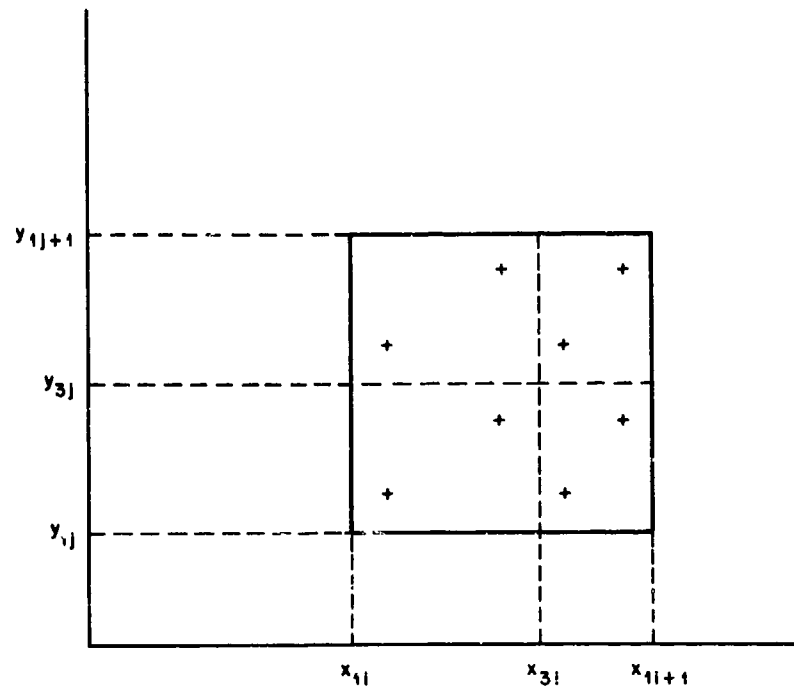


Fig. 4 — Initial positions of masses

$$M = (M_{01j} + M_{11-1j} + M_{31-1j-1} + M_{21j-1}) \quad (23)$$

where the first subscript on each M refers to a subcell (see Fig. 2b). The volume in which this mass is contained is given by

$$V = \frac{1}{2} (x_{31}^2 - x_{31-1}^2) (y_{3j} - y_{3j-1}) \quad (24)$$

Substituting in Eq. (17), we find that the density associated with the pressure is

$$\rho = \frac{(M_{01j} + M_{11-1j} + M_{31-1j-1} + M_{21j-1})}{\frac{1}{2} (x_{31}^2 - x_{31-1}^2) (y_{3j} - y_{3j-1})} \quad (25)$$

In a similar manner, the effective specific energy for the pressure computation becomes

$$e = \frac{M_{01j} e_{1j} + M_{11-1j} e_{1-1j} + M_{21j-1} e_{1j-1} + M_{31-1j-1} e_{1-1j-1}}{M_{01j} + M_{11-1j} + M_{21j-1} + M_{31-1j-1}} \quad (26)$$

Upon substitution of Eqs. (25) and (26) in the equation of state for the fluid, Eq. (11), the pressure  $P_{1j}$  is determined.

Certain boundary conditions affect the computation of pressure. For instance, at  $y_{1j} = 0$ , either Eqs. (23) through (26) must be modified to take into account the presence of the boundary, or mass and specific energy for fictitious cells below  $y = 0$  must be supplied. Similarly, some adjustment is needed along the axis of symmetry at  $x_{11} = 0$ . We choose to modify the equations rather than supply variables for the fictitious cells. Hence, at  $x_{11} = 0$ ,  $y_{1j} = 0$ , Eqs. (23) through (26) become

$$M = M_{01j} \quad (23a)$$

$$V = \frac{1}{2} \left( x_{3i}^2 \right) \left( y_{3j} \right) \quad (24a)$$

$$\rho = \frac{M_{01j}}{\frac{1}{2} x_{3i}^2 y_{3j}} \quad (25a)$$

$$e = e_{1j} \quad (26a)$$

where for this example  $x_{1i} = 0$ ,  $y_{1j} = 0$  when  $i = 1$  and  $j = 1$ . At  $x_{1i} \neq 0$ ,  $y_{1j} = 0$ , Eqs. (23) through (26) become

$$M = \left( M_{01j} + M_{1i-1j} \right) \quad (23b)$$

$$V = \frac{1}{2} \left( x_{3i}^2 - x_{3i-1}^2 \right) \left( y_{3j} \right) \quad (24b)$$

$$\rho = \frac{\left( M_{01j} + M_{1i-1j} \right)}{\frac{1}{2} \left( x_{3i}^2 - x_{3i-1}^2 \right) \left( y_{3j} \right)} \quad (25b)$$

$$e = \frac{M_{01j} e_{1j} + M_{1i-1j} e_{1-1j}}{M_{01j} + M_{1i-1j}} \quad (26b)$$

Finally, at  $x_{1i} = 0$ ,  $y_{1j} \neq 0$ , Eqs. (23) through (26) become

$$M = \left( M_{01j} + M_{21j-1} \right) \quad (23c)$$

$$V = \frac{1}{2} \left( x_{3i}^2 \right) \left( y_{3j} - y_{3j-1} \right) \quad (24c)$$

$$\rho = \frac{(M_{01j} + M_{21j-1})}{\frac{1}{2} x_{31}^2 (y_{3j} - y_{3j-1})} \quad (25c)$$

$$e = \frac{M_{01j} e_{1j} + M_{21j-1} e_{1j-1}}{M_{01j} + M_{21j-1}} \quad (26c)$$

Other types of boundary conditions require similar considerations. Free boundaries are such that the pressure must be zero on the boundary. This can be handled numerically by imposing the following restriction: If any  $M_{1j}$  is zero for the full cell corresponding to  $M_{ki,j}$  in Eqs. (23), (23a), (23b), or (23c), whichever is applicable, then the resulting pressure is zero; otherwise the computation of pressure is carried out as previously described.

This method of evaluating pressure from the equation of state is employed not only in the computation of initial conditions but also in subsequent computation in the integration process itself.

#### PRELIMINARY CALCULATION OF VELOCITY

The first step in the numerical integration of the equations is to estimate the new velocity in each cell. The x-component of Eq. (1) is written

$$\rho \frac{Du}{Dt} + \frac{\partial P}{\partial x} + \rho \frac{\partial \xi}{\partial x} = 0$$

which, for our example is

$$\rho \frac{Du}{Dt} + \frac{\partial P}{\partial x} = 0$$

since grad  $\phi$  in the x direction is zero. Neglecting the convective term and dividing by  $\rho$  we have

$$\frac{\partial u}{\partial t} = - \frac{1}{\rho} \frac{\partial P}{\partial x} \quad (27)$$

This equation requires  $\rho$  and  $\frac{\partial P}{\partial x}$  to be known in order to evaluate the change in the u component of velocity with respect to time. For the fluid model the density  $\rho$  is known in each cell, but  $\frac{\partial P}{\partial x}$  is not. We estimate  $\frac{\partial P}{\partial x}$  in the following manner.

Assuming that the pressure varies linearly from one corner of a cell to another, an average pressure  $\bar{P}$  for a face can be computed. For face 0 of cell ij the average pressure  $P_{0ij}^n$  is

$$P_{0ij}^n = \frac{1}{2} (P_{1j}^n + P_{1j+1}^n) \quad (28)$$

and for face 1 the average pressure  $P_{1ij}^n$  is

$$P_{1ij}^n = \frac{1}{2} (P_{1+1j}^n + P_{1+1j+1}^n) \quad (29)$$

If we approximate  $\frac{\partial P}{\partial x}$  with

$$\frac{\partial P}{\partial x} \sim \frac{P_{1ij}^n - P_{0ij}^n}{x_{11+1} - x_{11}}$$

and substitute this expression into Eq. (27), we have for the change in u in cell ij at time  $t_n$

$$u_{ij}^n = - \frac{1}{\rho_{ij}^n} \left( \frac{P_{1ij}^n - P_{0ij}^n}{x_{11+1} - x_{11}} \right) \quad (30)$$

where the dot denotes the time derivative  $\frac{\partial}{\partial t}$ . The pressures  $\bar{P}_{01j}^n$  and  $\bar{P}_{11j}^n$  are given by Eqs. (28) and (29) respectively, and  $\rho_{1j}^n$  is given by Eq. (17).

For the change in velocity in the y direction, the differential equation is

$$\rho \frac{Dv}{Dt} + \frac{\partial P}{\partial y} + 1 + \rho \frac{\partial \phi}{\partial y} = 0$$

which for our example may be written

$$\rho \frac{Dv}{Dt} + \frac{\partial P}{\partial y} + \rho g = 0$$

Again, we drop the convective term and divide by  $\rho$ , to obtain

$$\frac{\partial v}{\partial t} = -\frac{1}{\rho} \frac{\partial P}{\partial y} - g \quad (31)$$

Calculating average pressures in the manner stated above, we have for cell ij

$$v_{1j}^n = -\frac{1}{\rho_{1j}^n} \left( \frac{\bar{P}_{31j}^n - \bar{P}_{21j}^n}{y_{1j+1} - y_{1j}} \right) - g \quad (32)$$

where

$$\bar{P}_{21j}^n = \frac{1}{2} (P_{1j}^n + P_{1+1j}^n) \quad (33)$$

$$\bar{P}_{31j}^n = \frac{1}{2} (P_{1j+1}^n + P_{1+1j+1}^n) \quad (34)$$

If the change in velocity is assumed to be constant over the time step and equal to the value at the beginning of the time step,

the estimated velocities at  $t_{n+1}$  are

$$\tilde{u}_{ij}^{n+1} = u_{ij}^n + \Delta t_{n+1} \dot{u}_{ij}^n \quad (35)$$

$$\tilde{v}_{ij}^{n+1} = v_{ij}^n + \Delta t_{n+1} \dot{v}_{ij}^n$$

with  $\Delta t_{n+1} = t_{n+1} - t_n$ . Here the tilde denotes an estimate of velocity, since we have assumed that masses do not move. Also, the estimated average velocities for the time step are

$$\bar{u}_{ij}^{n+1} = \frac{1}{2} (u_{ij}^n + \tilde{u}_{ij}^{n+1}) \quad (36)$$

$$\bar{v}_{ij}^{n+1} = \frac{1}{2} (v_{ij}^n + \tilde{v}_{ij}^{n+1})$$

#### PRELIMINARY CALCULATION OF INTERNAL ENERGY

The next phase of the numerical process is concerned with the estimation of specific internal energy in each cell at the end of the time interval. The conservation-of-energy relation given by Eq. (9) serves as the basis for this computation. Since we assume that density, velocity, and specific internal energy are constant over the cell, and  $\text{grad } \phi$  is also constant, Eq. (9) may be written

$$\rho V \vec{u} \cdot \text{grad } \phi + \rho V \frac{D}{Dt} \left( \frac{1}{2} \vec{u} \cdot \vec{u} + e \right) = - \int_S \vec{P} \vec{u} \cdot d\vec{S}$$

Dropping the convective term and dividing by  $\rho V$ , we have for the change in specific energy

$$\frac{\partial e}{\partial t} = -\vec{u} \cdot \text{grad } \phi - \frac{\partial}{\partial t} \left( \frac{1}{2} \vec{u} \cdot \vec{u} \right) - \frac{1}{\rho V} \int_S \vec{P} \vec{u} \cdot d\vec{S} \quad (37)$$



Integrating Eq. (37) with respect to time yields the change in specific energy for the time interval, which, when added to the specific energy at the beginning of the interval, results in the desired estimate of specific energy. Because of this integration with respect to time, average velocity for the time step is used wherever velocity is required in evaluating Eq. (37).

For the physical example where  $\text{grad } \phi$  is given by Eq. (19), the first term in Eq. (37) is

$$-\vec{u} \cdot \text{grad } \phi = -\bar{g}_{1j}^{n+1} \quad (38)$$

and the second term is

$$-\frac{\partial}{\partial t} \left( \frac{1}{2} \vec{u} \cdot \vec{u} \right) = -\bar{u}_{1j}^{n+1} u_{1j}^n - \bar{v}_{1j}^{n+1} v_{1j}^n \quad (39)$$

The mass  $\rho V$  in the third term in Eq. (36) is equal to  $\rho_{1j}^n V_{1j}$ , while the integral represents the rate at which the energy is being diminished by work done on the surface of the volume element. In evaluating the surface work integral for a cell we note that the volume element under consideration has six different surfaces. Only four of these, however, contribute to the integral since the net work done on the surfaces coincident with the meridian planes is zero due to cylindrical symmetry. Integrals for the four other surfaces (0, 1, 2, 3) which do contribute are evaluated separately then summed to determine the total integral.

To evaluate each of these integrals, we first determine the quantity  $\vec{P} \cdot d\vec{S}$  and then integrate. For face 01j the pressure  $P$

Integrating Eq. (37) with respect to time yields the change in specific energy for the time interval, which, when added to the specific energy at the beginning of the interval, results in the desired estimate of specific energy. Because of this integration with respect to time, average velocity for the time step is used wherever velocity is required in evaluating Eq. (37).

For the physical example where  $\text{grad } \phi$  is given by Eq. (19), the first term in Eq. (37) is

$$-\vec{u} \cdot \text{grad } \phi = -g\bar{v}_{1j}^{n+1} \quad (38)$$

and the second term is

$$-\frac{\partial}{\partial t} \left( \frac{1}{2} \vec{u} \cdot \vec{u} \right) = -\bar{v}_{1j}^{n+1} \bar{v}_{1j}^n - \bar{v}_{1j}^{n+1} \bar{v}_{1j}^n \quad (39)$$

The mass  $\rho V$  in the third term in Eq. (36) is equal to  $\rho_{1j}^n V_{1j}$  and the integral represents the rate at which the energy is being diminished by work done on the surface of the volume element. In evaluating the surface work integral for a cell we note that the volume element under consideration has six different surfaces. Only four of these, however, contribute to the integral since the net work done on the surfaces incident with the meridian planes is zero due to cylindrical symmetry. Integrals for the four other surfaces (0, 1, 2, 3) which do contribute are evaluated separately then summed to determine the total integral.

To evaluate each of these integrals, we first determine the quantity  $\vec{P} \cdot \vec{dS}$  and then integrate. For face 01j the pressure  $P$

is a function of  $y$  alone as given in Eq. (16). The function  $\vec{u} \cdot d\vec{S}$  represents the velocity normal to the surface (and taken to be positive in the outward sense) times the element of area over which it acts. Since we consider the velocity in each cell to be constant over the cell, a discontinuous velocity at a surface common to two cells can occur if the velocities in those cells are different. Hence the following assumption is made: The velocity on such a common surface is equal to the average of the velocities in the adjacent cells. The function  $\vec{u} \cdot d\vec{S}$  may now be evaluated; for face 0 it is

$$\vec{u} \cdot d\vec{S} = -\frac{1}{2} \left( \bar{u}_{1-1j}^{n+1} + \bar{u}_{1j}^{n+1} \right) \left( x_{11} dy \right) \quad (40)$$

The negative sign appears because of the outward sense of the normal. Upon substitutions of Eqs. (18) and (40) we find for this one face

$$-\int_S \vec{P}\vec{u} \cdot d\vec{S} = \frac{1}{2} \int_{y_{1j}}^{y_{1j+1}} \left[ P_{1j}^n + \frac{y - y_{1j}}{y_{1j+1} - y_{1j}} \left( P_{1j+1}^n - P_{1j}^n \right) \right] \left[ \bar{u}_{1-1j}^{n+1} + \bar{u}_{1j}^{n+1} \right] x_{11} dy$$

which after integration becomes

$$-\int_S \vec{P}\vec{u} \cdot d\vec{S} = \frac{x_{11}}{4} \left( y_{1j+1} - y_{1j} \right) \left( P_{1j}^n + P_{1j+1}^n \right) \left( \bar{u}_{1-1j}^{n+1} + \bar{u}_{1j}^{n+1} \right) \quad (41)$$

Proceeding in a similar manner for the opposite face,  $11j$ , we find that the integral of Eq. (37) is

$$-\int_S \vec{P}\vec{u} \cdot d\vec{S} = -\frac{x_{11+1}}{4} \left( y_{1j+1} - y_{1j} \right) \left( P_{1+1j}^n + P_{1+1j+1}^n \right) \left( \bar{u}_{1j}^{n+1} + \bar{u}_{1+1j}^{n+1} \right) \quad (42)$$

Next, the pressure along face 2ij is given by

$$P_{2ij}^n = P_{1j}^n + \frac{x - x_{1i}}{x_{1i+1} - x_{1i}} \left( P_{i+1j}^n - P_{1j}^n \right) \quad (43)$$

and the function  $\vec{u} \cdot d\vec{S}$  in the outward sense is

$$-\vec{u} \cdot d\vec{S} = -\frac{1}{2} \left( \bar{v}_{1j-1}^{n+1} + \bar{v}_{1j}^{n+1} \right) x \, dx \quad (44)$$

Substituting for the integral, we have

$$-\int_S \vec{P} \cdot d\vec{S} = \frac{1}{2} \int_{x_{1i}}^{x_{1i+1}} P_{2ij}^n \left( \bar{v}_{1j-1}^{n+1} + \bar{v}_{1j}^{n+1} \right) x \, dx$$

which after integration becomes

$$\begin{aligned} -\int_S \vec{P} \cdot d\vec{S} = & + \frac{1}{12} \left( x_{1i+1} - x_{1i} \right) \left( \bar{v}_{1j-1}^{n+1} + \bar{v}_{1j}^{n+1} \right) \left[ P_{1j}^n \left( 2x_{1i} + x_{1i+1} \right) \right. \\ & \left. + P_{i+1j}^n \left( x_{1i} + 2x_{1i+1} \right) \right] \end{aligned} \quad (45)$$

In a similar fashion for the integral for the opposite face, 3ij, is

$$\begin{aligned} -\int_S \vec{P} \cdot d\vec{S} = & - \frac{1}{12} \left( x_{1i+1} - x_{1i} \right) \left( \bar{v}_{1j}^{n+1} + \bar{v}_{1j+1}^{n+1} \right) \left[ P_{1j+1}^n \left( 2x_{1i} + x_{1i+1} \right) \right. \\ & \left. + P_{i+1j+1}^n \left( x_{1i} + 2x_{1i+1} \right) \right] \end{aligned} \quad (46)$$

The total integral in Eq. (37) is the sum of the integrals for the four faces given by Eqs. (41), (42), (45), and (46).

It should be noted that when one cell receives an increment of energy,  $\vec{P} \cdot d\vec{S} \, \Delta t$ , exactly that amount is subtracted from the

appropriate adjoining cell, so that total energy is conserved. Since the repartitioning process discussed in the following sections also conserves energy, the external potential,  $\Phi$ , is the only agency which can cause a change in the total energy. In cases where  $\Phi = 0$ , this provides a valuable check on the computation.

The change in specific energy per unit time, Eq. (37), may now be evaluated using Eqs. (38), (39), (41), (42), (45), and (46) with  $\rho V = \rho_{ij}^n V_{ij}$ . Integrating with respect to time we find

$$\begin{aligned} \bar{e}_{ij}^{n+1} = e_{ij}^n - \Delta t_{n+1} g \bar{v}_{ij}^{n+1} - \Delta t_{n+1} \left( \bar{u}_{ij}^{n+1} \bar{u}_{ij}^n + \bar{v}_{ij}^{n+1} \bar{v}_{ij}^n \right) \\ - \frac{\Delta t_{n+1}}{\rho_{ij}^n V_{ij}} \left[ \frac{(y_{1,j+1} - y_{1j})}{4} \left\{ x_{1i+1} (p_{i+1j}^n + p_{i+1,j+1}^n) (\bar{u}_{ij}^{n+1} + \bar{u}_{i+1j}^{n+1}) \right. \right. \\ \left. \left. - x_{1i} (p_{ij}^n + p_{i,j+1}^n) (\bar{u}_{i-1j}^{n+1} + \bar{u}_{ij}^{n+1}) \right\} \right. \\ \left. + \frac{(x_{1i+1} - x_{1i})}{12} \left\{ (\bar{v}_{ij}^{n+1} + \bar{v}_{i,j+1}^{n+1}) (p_{i,j+1}^n \{2x_{1i} + x_{1i+1}\} \right. \right. \\ \left. \left. + p_{i+1,j+1}^n \{x_{1i} + 2x_{1i+1}\}) - (\bar{v}_{i,j-1}^{n+1} + \bar{v}_{ij}^{n+1}) \right\} \right. \\ \left. \left. + \left( p_{ij}^n \{2x_{1i} + x_{1i+1}\} + p_{i+1j}^n \{x_{1i} + 2x_{1i+1}\} \right) \right] \right] \quad (47) \end{aligned}$$

In Eq. (47) no account has been taken of the effect of boundary conditions other than the presence of free boundaries where the pressure is zero (as discussed previously). In our particular example no work can be done on the fixed boundary or on the boundary of symmetry because the velocity normal to these boundaries is zero. Hence the term in Eq. (47) resulting from Eq. (45) is zero for  $y_{1j} = 0$ , and the term resulting from Eq. (41) is zero when  $x_{1i} = 0$ .

Having computed the estimates for the velocity and specific internal energy at time  $t_{n+1}$ , we can determine the momentum in each direction and the sum of the kinetic and internal energy for each cell. The momentum in the x and y directions, respectively, are

$$\begin{aligned} \text{Momentum}_x &= M_{ij}^n \tilde{u}_{ij}^{n+1} \\ \text{Momentum}_y &= M_{ij}^n \tilde{v}_{ij}^{n+1} \end{aligned} \quad (48)$$

where

$$M_{ij}^n = \rho_{ij}^n V_{ij}$$

The estimated kinetic plus internal energy in a cell is

$$M_{ij}^n \left( \tilde{e}_{ij}^{n+1} + \frac{1}{2} \left( \tilde{u}_{ij}^{n+1} \right)^2 + \frac{1}{2} \left( \tilde{v}_{ij}^{n+1} \right)^2 \right) \quad (49)$$

Expressions (48) and (49) are correct at the end of the time interval, provided no mass changes location from one cell to another (i.e.,  $M_{ij}^{n+1} = M_{ij}^n$ ). To correct these estimates of momentum and energy for cells which do not meet this condition, each mass which changes cells is considered to carry with it to the new cell its share of the momentum and kinetic plus internal energy. This together with the integration of Eq. (37) insures that mass, momentum, and total energy (kinetic + internal + potential) are all conserved.

#### MASS MOVEMENT

In the next phase of the computation, the masses are moved

according to an average velocity for the time cycle. First the subscripts p and q are determined such that

$$x_{2p-1} \leq x_m^n < x_{2p} \quad (50)$$

$$y_{2q-1} \leq y_m^n < y_{2q}$$

where  $x_m^n$  and  $y_m^n$  define the position of the  $m^{\text{th}}$  mass point at time  $t_n$  and  $x_{2p}$  and  $y_{2q}$  define the center of area of the cell pq. The velocity of the mass thus located is considered to be a sum of the velocities in cells p-1 q-1, p q-1, p-1 q, and p q weighted, respectively, by  $a_0$ ,  $a_1$ ,  $a_2$ , and  $a_3$

$$\bar{u}_m^{n+1} = a_0 \bar{u}_{p-1q-1}^{n+1} + a_1 \bar{u}_{pq-1}^{n+1} + a_2 \bar{u}_{p-1q}^{n+1} + a_3 \bar{u}_{pq}^{n+1} \quad (51)$$

$$\bar{v}_m^{n+1} = a_0 \bar{v}_{p-1q-1}^{n+1} + a_1 \bar{v}_{pq-1}^{n+1} + a_2 \bar{v}_{p-1q}^{n+1} + a_3 \bar{v}_{pq}^{n+1}$$

where  $\bar{u}_m^{n+1}$  and  $\bar{v}_m^{n+1}$  are the migration velocities assigned to the  $m^{\text{th}}$  mass point in the x and y directions, respectively. The weights are determined in the following fashion: First the proportional areas  $c_0$ ,  $c_1$ ,  $c_2$ , and  $c_3$  are computed

$$c_0 = \left( \frac{x_{2p} - x_m^n}{x_{2p} - x_{2p-1}} \right) \left( \frac{y_{2q} - y_m^n}{y_{2q} - y_{2q-1}} \right)$$

$$c_1 = \left( \frac{x_m^n - x_{2p-1}}{x_{2p} - x_{2p-1}} \right) \left( \frac{y_{2q} - y_m^n}{y_{2q} - y_{2q-1}} \right)$$

$$c_2 = \left( \frac{y_{2p}^n - x_m^n}{x_{2p}^n - x_{2p-1}^n} \right) \left( \frac{y_m^n - y_{2q-1}^n}{y_{2q}^n - y_{2q-1}^n} \right)$$

$$c_3 = \left( \frac{x_m^n - x_{2p-1}^n}{x_{2p}^n - x_{2p-1}^n} \right) \left( \frac{y_m^n - y_{2q-1}^n}{y_{2q}^n - y_{2q-1}^n} \right) \quad (52)$$

Next  $b_0$ ,  $b_1$ ,  $b_2$ , and  $b_3$  are determined\*

$$b_0 = c_0 \quad M_{p-1q-1}^n \neq 0$$

$$b_0 = 0 \quad M_{p-1q-1}^n = 0$$

$$b_1 = c_1 \quad M_{pq-1}^n \neq 0$$

$$b_1 = 0 \quad M_{pq-1}^n = 0$$

$$b_2 = c_2 \quad M_{p-1q}^n \neq 0$$

$$b_2 = 0 \quad M_{p-1q}^n = 0$$

$$b_3 = c_3 \quad M_{pq}^n \neq 0$$

$$b_3 = 0 \quad M_{pq}^n = 0$$

(53)

---

\*In order to avoid certain difficulties on cells adjacent to free surfaces, it is helpful to use an alternate scheme for computing  $(b_0, b_1, b_2, b_3)$ . In the alternate method, we use  $b_0 = C_0 M_{p-1q-1}^n$ , etc.



Finally, the weights  $a_0$ ,  $a_1$ ,  $a_2$ , and  $a_3$  are defined

$$\begin{aligned} a_0 &= \frac{b_0}{b_0 + b_1 + b_2 + b_3} \\ a_1 &= \frac{b_1}{b_0 + b_1 + b_2 + b_3} \\ a_2 &= \frac{b_2}{b_0 + b_1 + b_2 + b_3} \\ a_3 &= \frac{b_3}{b_0 + b_1 + b_2 + b_3} \end{aligned} \tag{54}$$

Substituting Eqs. (54) in Eqs. (51) yields the average velocity for the time cycle for mass  $m$ .

Again, boundary conditions modify the computation of velocity. For the fixed boundary at  $y = 0$ , cells  $p-1$   $q-1$  and  $p$   $q-1$  represent fictitious cells. The determination of the velocity near this boundary is achieved by modifying the computation of the  $c$ 's of Eqs. (52)

$$\begin{aligned} c_0 &= 0 \\ c_1 &= 0 \\ c_2 &= \left( \frac{x_{2p}^n - x_m^n}{x_{2p}^n - x_{2p-1}^n} \right) \left( \frac{y_m^n}{y_{2q}^n} \right) \\ c_3 &= \left( \frac{x_m^n - x_{2p-1}^n}{x_{2p}^n - x_{2p-1}^n} \right) \left( \frac{y_m^n}{y_{2q}^n} \right) \end{aligned} \tag{52a}$$

Substitution of Eqs. (52a) in Eqs. (52) and continuing in the manner previously described permit the velocity of the mass near the boundary to be determined.

Similarly, for the velocity near the boundary of symmetry, the  $c$ 's are computed in the following manner.

$$c_0 = 0$$

$$c_1 = \left( \frac{x_m^n}{x_{2p}} \right) \left( \frac{y_{2q}^n - y_m^n}{y_{2q} - y_{2q-1}} \right)$$

$$c_2 = 0 \quad (52b)$$

$$c_3 = \left( \frac{x_m^n}{x_{2p}} \right) \left( \frac{y_m^n - y_{2q-1}^n}{y_{2q} - y_{2q-1}} \right)$$

For the velocity near  $x = 0$  and  $y = 0$  the  $c$ 's are

$$c_0 = 0$$

$$c_1 = 0$$

(52c)

$$c_2 = 0$$

$$c_3 = \left( \frac{x_m^n}{x_{2p}} \right) \left( \frac{y_m^n}{y_{2q}} \right)$$

The new location of the mass, given by  $x_m^{n+1}$  and  $y_m^{n+1}$ , is determined by integrating Eqs. (51) with respect to time

$$\begin{aligned}x_m^{n+1} &= x_m^n + \Delta t_{n+1} u_m^{n+1} \\y_m^{n+1} &= y_m^n + \Delta t_{n+1} v_m^{n+1}\end{aligned}\tag{55}$$

Furthermore, we impose boundary conditions at  $x = 0$  and at  $y = 0$  such that no mass can cross the boundary. Thus if  $x_m^{n+1} < 0$ ,  $x_m^{n+1}$  is set equal to  $|x_m^{n+1}|$ ; similarly, if  $y_m^{n+1} < 0$ ,  $y_m^{n+1}$  is set equal to  $|y_m^{n+1}|$ . The  $m^{\text{th}}$  mass point at time  $t_n$  is in cell  $i_m^n j_m^n$ , where  $i_m^n$  and  $j_m^n$  are defined as

$$i_m^n = i \quad \text{when } x_{1i}^n \leq x_m^n < x_{1i+1}^n\tag{56}$$

$$j_m^n = j \quad \text{when } y_{1j}^n \leq y_m^n < y_{1j+1}^n$$

If at time  $t_{n+1}$ ,  $i_m^{n+1}$  and  $j_m^{n+1}$ , determined by substituting  $x_m^{n+1}$  and  $y_m^{n+1}$  for  $x_m^n$  and  $y_m^n$  in Eq. (56), are equal to  $i_m^n$  and  $j_m^n$ , respectively, no adjustment in momentum and energy is required since the mass does not change cells. If, however, the mass does change cells, then estimates of momentum and energy in both the old cell and the new cell are modified. The estimated momentum of the  $m^{\text{th}}$  mass point for the time interval  $t_n \leq t \leq t_{n+1}$  is, in the  $x$  direction and  $y$  direction, respectively

$$M_m \tilde{u}_{ij}^{n+1} \text{ and } M_m \tilde{v}_{ij}^{n+1}\tag{57}$$

where  $M_m$  is the mass of the  $m^{\text{th}}$  mass point, the estimated total energy assigned to this same mass point is

$$\frac{M_m}{M_{ij}^n} \left\{ \tilde{\Gamma}_{ij}^{n+1} + \frac{M_{ij}^n}{2} \left( \tilde{u}_{ij}^{n+1^2} + \tilde{v}_{ij}^{n+1^2} \right) \right\} \quad (58)$$

where  $\tilde{\Gamma}_{ij}^{n+1} = M_{ij}^n \tilde{e}_{ij}^{n+1}$ . The total mass in the  $ij^{th}$  cell at time  $t_n$  is  $M_{ij}^n$ , and  $\tilde{\Gamma}_{ij}^{n+1}$  is the total estimated internal energy for this same cell before mass movement. Notice that  $i = i_m^n$  and  $j = j_m^n$  in both Eqs. (57) and (58). In going from cell  $i_m^n j_m^n$  to  $i_m^{n+1} j_m^{n+1}$  the mass takes with it both momentum and energy. Hence expressions (57) and (58) are subtracted from the estimated momentum and kinetic plus internal energy for cell  $i_m^n j_m^n$  and added to those of cell  $i_m^{n+1} j_m^{n+1}$  for each mass point which crosses from cell  $i_m^n j_m^n$  to cell  $i_m^{n+1} j_m^{n+1}$ .

#### REPARTITIONING

After all of the masses have been moved and the total estimated momentum and energy for the cells have been adjusted correspondingly, a final set of values for density, velocity, and specific internal energy at time  $n+1$  must be assigned to each cell. These values are chosen so that the total mass, momentum, and energy assigned to each cell after mass movement are conserved.

First, the mass  $M_{ij}^{n+1}$  of the  $ij^{th}$  cell after mass movement is found by simply adding up the masses of all of the individual mass points in the  $ij^{th}$  cell at this phase of the calculation. The new density of the cell is then given by

$$\rho_{ij}^{n+1} = \frac{M_{ij}^{n+1}}{V_{ij}} \quad (59a)$$

The new velocities  $(u_{ij}^{n+1}, v_{ij}^{n+1})$  are given respectively by

$$u_{ij}^{n+1} = \frac{[\text{Total estimated momentum, x direction}]_{ij}}{M_{ij}^{n+1}} \quad (59b)$$

$$v_{ij}^{n+1} = \frac{[\text{Total estimated momentum, y direction}]_{ij}}{M_{ij}^{n+1}} \quad (59c)$$

$$e_{ij}^{n+1} = \frac{[\text{Total estimated energy}]_{ij} - \frac{1}{2} M_{ij}^{n+1} [(u_{ij}^{n+1})^2 + (v_{ij}^{n+1})^2]}{M_{ij}^{n+1}} \quad (59d)$$

#### PRESSURE CALCULATION

The final step in the numerical integration process is to compute the pressures  $P_{ij}^{n+1}$  as described in Section IV using the new values of specific internal energy  $e_{ij}^{n+1}$  and density  $\rho_{ij}^{n+1}$ .

#### STABILITY CHECK

Together with the computation of the internal pressures it is desirable to perform a check on the stability of the numerical integration process. At the present time, there appears to be no stability criterion specifically designed for the PIC process, although the von Neumann method<sup>(11)</sup> of stability analysis used in association with the existing PIC analogue difference equations<sup>(4,8)</sup> could probably be used to develop one. A rough approximation to a stability criterion is given by the conditions that the mesh speed in any direction should exceed the speed of a sound wave (relative to a fixed reference frame) in that direction. For our problem this condition becomes,

$$\Delta t < \text{Min} \left\{ \frac{\Delta x}{|u| + v_s}, \frac{\Delta y}{|v| + v_s} \right\}$$

where  $\Delta x$  and  $\Delta y$  are increments of Eulerian coordinates and  $v_s$  is the local velocity of sound of an observer moving with the fluid.

This condition is always met by

$$\Delta t < \text{Min} \frac{\{\Delta x, \Delta y\}}{v_s + \sqrt{u^2 + v^2}}$$

For practical computations we have found that

$$\sqrt{u^2 + v^2} \leq v_s$$

We therefore choose as our stability criterion

$$\Delta t = \frac{\{\Delta x, \Delta y\} \min}{r v_s} \quad (60)$$

where  $r$  is a constant (approximately equal to 2) that is generally established by preliminary computational experiments for whatever problem we have in mind.

The velocity of sound is given by

$$v_s^2 = \left( \frac{\partial P}{\partial \rho} \right)_s \quad (61)$$

that is, the partial derivative of  $P$  with respect to  $\rho$  at constant entropy. Since at constant entropy

$$de = \frac{P}{\rho^2} d\rho$$

then

$$v_s^2 = \left( \frac{\partial P}{\partial \rho} \right)_e + \frac{P}{\rho} \left( \frac{\partial P}{\partial e} \right)_\rho \quad (62)$$

For stability of the numerical process to be assured, the Courant condition, Eq. (60), is observed throughout the region. In the case of the equation of state given by Eq. (10) we have

$$v_s^2 = \gamma \frac{P}{\rho} \quad (63)$$

Therefore for each point in the fluid at which pressure is computed the condition to be satisfied is

$$s = r \left( \gamma \frac{P}{\rho} \right) \left( \frac{\Delta t_{n+1}}{\min(\Delta x, \Delta y)} \right)^2 \leq 1 \quad (64)$$

In addition to a check on stability we may use Eq. (64) to adjust the time interval during the course of integration so that an optimum time interval is always used. This is done in the following manner

$$\Delta t_{n+2} = \Delta t_{n+1} \quad \text{for } s_1 \leq s \leq s_2 < 1$$

$$\Delta t_{n+2} = r_1 \Delta t_{n+1} \quad \text{for } s < s_1 \quad (r_1 > 1)$$

$$\Delta t_{n+2} = r_2 \Delta t_{n+1} \quad \text{for } s_2 < s \quad (r_2 < 1)$$

That is, if the calculated value of the stability function  $s$  at time  $t_{n+1}$  lies between or on either of two preassigned numbers,  $s < s_2 < 1$ , then the subsequent time interval is not changed. If the stability

function  $s$  is less than  $s_1$ , then the time interval is increased by a multiplier  $r_1$ . If  $s$  is greater than  $s_2$ , however, the time interval is decreased by the multiplier  $r_2$ . The numbers  $r_1$  and  $r_2$  are also positive preassigned constants.

#### GRID CHANGE

Sooner or later the disturbance induced by the presence of the blast will reach the grid boundary at  $x = x_{\max}$ ,  $y = y_{\max}$ , or both. At this point in time, computation with the current model must cease, because the material will soon flow to nonexistent cells and further computations will become meaningless. Consequently, at the end of each integration step, tests are made to determine whether or not the disturbance has reached the boundary. These tests involve a search for nonzero velocity and for specific internal energy, density, or pressures which are different from their original values in any cell adjacent to the boundary.

In instances where disturbances spread through a larger and larger volume of material, it is often desirable to maintain at all times a high degree of resolution with respect to the disturbed volume. The airburst problem is one such case. At the time when a disturbance reaches the assumed boundary in the example, it is possible to create a new model with the characteristics of the old model at that specific time, so that integration can be resumed. This is done in the following manner.

The new region is selected in such a way that all the fluid in the old model is contained within the volume of the new model. Such selection for our physical example is illustrated in Fig. 5. Here



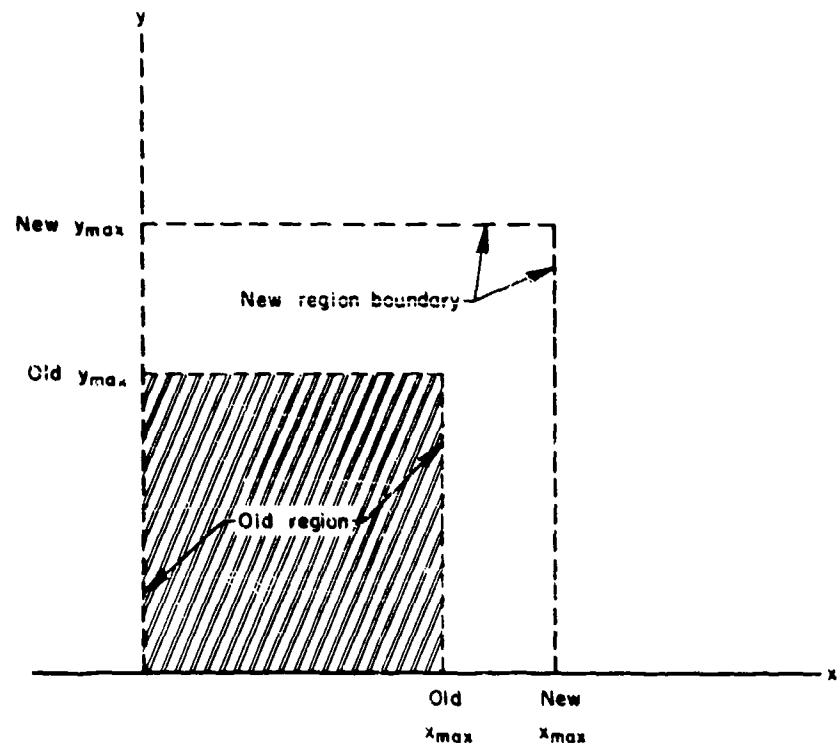


Fig. 5 — New and old regions in transfer

the maximum dimensions of the new region are at "new"  $x_{\max}$  and "new"  $y_{\max}$ ; the old region is completely enclosed in the new region.

The new region is then subdivided into volume elements in the same manner as described before. Mass, momentum, and energy are now assigned to the cells of the whole new region in two distinct steps: First to those cells or parts of cells which coincide with the new region, and then to those cells or parts of cells which coincide with the old region. Initial values of mass, kinetic plus internal energy, and momentum are provided in the new cells for the additional fluid which has been encompassed; i.e., in the new cells where  $x_{1i+1} > \text{"old" } x_{\max}$ , or  $y_{1j+1} > \text{"old" } y_{\max}$ . Here it is possible that a given cell may encompass some old volume as well as some new volume of fluid. In this event, the mass, energy, and momentum for the new fluid only are provided in these cells.

Next the mass of the fluid in each cell of the old region is added to the proper new cells, as shown in Fig. 6, under the assumption of uniform density for each old cell. The portion of mass of the old cell which is contained in the new cell 1 is added to the mass in new cell 1. Similarly the kinetic plus internal energy and momentum associated with mass  $M_1$  are added to the energy and momentum in new cell 1. The other new cells, 2, 3, and 4, receive mass  $M_2$ ,  $M_3$ , and  $M_4$ , respectively, from the old cells and also receive the corresponding portions of energy and momentum.

After all the mass, energy, and momentum in the old cells have been redistributed to the new cells, the velocity, specific energy, and density are computed in the new cells in the manner described in

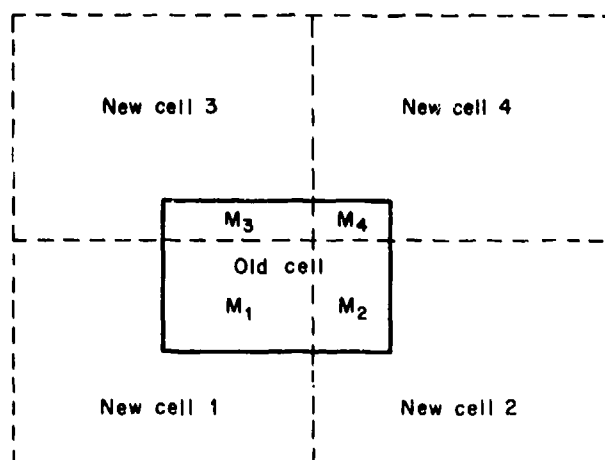


Fig 6 — Contribution of mass by old cell to new cell

Section IV. The mass in each cell is then divided equally among a number of mass points, positioned so that the density is approximately uniform.

Finally the pressure at the corners of the cell is computed from the equation of state of the fluid using the method detailed in Section IV.

The variables associated with the new cells are the initial conditions for continuing the integration. As time goes on, subsequent grid changes may be necessary to obtain the desired solution to the physical problem.

The grid change provides a means by which we can overlay on a given network one of less detail, while conserving mass, momentum, and energy. Some loss of detail occurs, to be sure, but the general characteristics of the old region are carried over into the new region.

REFERENCES

1. Bjork, R. L., Effects of a Meteoroid Impact on Steel and Aluminum in Space, The RAND Corporation, P-1662, December 1958.
2. Brode, H. L., and R. L. Bjork, Cratering From a Megaton Surface Burst, The RAND Corporation, RM-2600, June 30, 1960.
3. Courant, R., and K. O. Friedrichs, Supersonic Flow and Shock Waves, Interscience Publishers, Inc., New York, 1948.
4. Harlow, F. H., and M. Evans, The Particle-In-Cell Method for Hydrodynamic Calculations, Los Alamos Scientific Laboratory, LA-2139, November 1957.
5. Harlow, F. H., "The Particle-In-Cell Method for Numerical Solution of Problems on Fluid Mechanics," to be published in the Proceedings of the Symposium on Experimental Arithmetic.
6. Harlow, F. H., Two-Dimensional Hydrodynamic Calculations, Los Alamos Scientific Laboratory, LA-2301, September 1959.
7. Harlow, F. H., "Hydrodynamic Problems Involving Large Fluid Distortions," J. Assoc. Computing Machinery, Vol. 4, No. 2, April 1957, pp. 137-142.
8. Papetti, R., A Particle-In-Cell Error Analysis, The RAND Corporation, RM-3613-PR (to be published).
9. Von Neumann, J., and R. D. Richtmyer, "A Method for the Numerical Calculation of Hydrodynamic Shocks," J. Appl. Phys., Vol. 21, No. 3, March 1950, pp. 232-237.
10. Brode, H., Point Source Explosion in Air, The RAND Corporation, RM-1824-AEC, December 1955.
11. Richtmyer, R. D., Difference Methods for Initial-Value Problems, Interscience Tracts in Pure and Applied Mathematics, No. 4, Interscience Publishers, Inc., New York, 1957.